Dysregulation of *Escherichia coli* α-hemolysin expression alters the course of acute and persistent urinary tract infection

Kanna Nagamatsu[a], Thomas J. Hannan[b], Randi L. Guest[c], Maria Kostakioti[a,1], Maria Hadjifrangiskou[a,d], Jana Binkley[a], Karen Dodson[a], Tracy L. Raivio[c], and Scott J. Hultgren[a,e,2]

Departments of [a]Molecular Microbiology and Microbial Pathogenesis and [b]Pathology and Immunology, [e]Center for Women's Infections Disease Research, Washington University School of Medicine, St. Louis, MO 63110; [c]Department of Biological Sciences, University of Alberta, Edmonton, AB, Canada T6G 2E9; and [d]Department of Pathology, Microbiology, and Immunology, Vanderbilt University School of Medicine, Nashville, TN 37232

Contributed by Scott J. Hultgren, January 14, 2015 (sent for review September 10, 2014)

Urinary tract infections (UTIs) are among the most common bacterial infections, causing considerable morbidity in females. Infection is highly recurrent despite appropriate antibiotic treatment. Uropathogenic *Escherichia coli* (UPEC), the most common causative agent of UTIs, invades bladder epithelial cells (BECs) and develops into clonal intracellular bacterial communities (IBCs). Upon maturation, IBCs disperse, with bacteria spreading to neighboring BECs to repeat this cycle. This process allows UPEC to gain a foothold in the face of innate defense mechanisms, including micturition, epithelial exfoliation, and the influx of polymorphonuclear leukocytes. Here, we investigated the mechanism and dynamics of urothelial exfoliation in the early acute stages of infection. We show that UPEC α-hemolysin (HlyA) induces Caspase-1/Caspase-4–dependent inflammatory cell death in human urothelial cells, and we demonstrate that the response regulator (CpxR)-sensor kinase (CpxA) two-component system (CpxRA), which regulates virulence gene expression in response to environmental signals, is critical for fine-tuning HlyA cytotoxicity. Deletion of the *cpxR* transcriptional response regulator derepresses *hlyA* expression, leading to enhanced Caspase-1/Caspase-4– and NOD-like receptor family, pyrin domain containing 3-dependent inflammatory cell death in human urothelial cells. In vivo, overexpression of HlyA during acute bladder infection induces more rapid and extensive exfoliation and reduced bladder bacterial burdens. Bladder fitness is restored fully by inhibition of Caspase-1 and Caspase-11, the murine homolog of Caspase-4. Thus, we have discovered that fine-tuning of HlyA expression by the CpxRA system is critical for enhancing UPEC fitness in the urinary bladder. These results have significant implications for our understanding of how UPEC establishes persistent colonization.

microbial pathogenesis | urinary tract infection | uropathogenic *E. coli* | persistent colonization

The vast majority of urinary tract infections (UTIs) are caused by uropathogenic *Escherichia coli* (UPEC) (1). UPEC is able to bind and invade bladder epithelial (urothelial) cells, where it is either expelled (2) or escapes to the cytoplasm, where it can replicate to high levels, forming intracellular bacterial communities (IBCs) (3, 4). Upon IBC maturation, the first round of which occurs during the first 12–16 h of infection, the bacteria detach from the biomass and flux back into the lumen, spreading to neighboring epithelial cells, where they are capable of initiating another IBC cycle (5). The exfoliation of superficial facet cells and regeneration of the urothelium in response to infection with UPEC can function to clear adherent and intracellular bacteria (4, 6), but may also promote the dissemination of UPEC into deeper layers of the urothelium, leading to chronic cystitis or enhanced formation of quiescent intracellular reservoirs (QIRs) that can seed recurrence (7, 8). Consequently, the shedding of urothelial cells can be viewed as a double-edged sword, potentially benefiting both host and pathogen. Although the exfoliation response was previously shown to be dependent upon the function of Caspases (4), the specific host and bacterial factors that modulate bladder cell death and exfoliation during the course of a UTI remain poorly understood.

Approximately 40–50% of *E. coli* isolated from patients with a UTI encodes a secreted pore-forming toxin known as α-hemolysin (HlyA) (9). Expression of HlyA in UPEC has been previously implicated in urothelial cell toxicity in vitro (10, 11) and increased urothelial damage in vivo (12). HlyA can form pores in the membranes and lyse a number of mammalian cell types, including RBCs (13). Recent studies have shown that HlyA can trigger rapid degradation of paxillin and other host proteins involved in cell–cell and cell–matrix interactions, a mechanism thought to promote exfoliation (14). In *Staphylococcus aureus*, hemolysins in the presence of lipoproteins promote the activation of Caspase-1 via the inflammasome in monocytic cells (15). However, the mechanism by which UPEC HlyA modulates host immune responses remains poorly understood.

Cells can die through distinct biochemical pathways that produce different morphological and physiological outcomes. Some cell death pathways involve a family of 14 tightly regulated cysteine proteases called Caspases. Apoptosis is a cell death program that occurs in the absence of inflammation (16) and involves two groups of Caspases: the initiator Caspases (i.e., Caspase-2, Caspase-8, Caspase-9, Caspase-10) and effector Caspases (i.e., Caspase-3, Caspase-6, Caspase-7) (17). The initiator Caspases are mediators

Significance

The majority of urinary tract infections (UTIs) are caused by uropathogenic *Escherichia coli* (UPEC). Upon UPEC infection, exfoliation of host bladder epithelial (urothelial) cells leads to sloughing of bacteria-laden cells into the urine for expulsion. However, it can also facilitate bacterial dissemination into deeper tissues. Thus, the balance and timing of exfoliation are important in determining disease outcomes. Here, we investigate host–pathogen dynamics in human urothelial cells in vitro and in murine model of acute cystitis. We discovered that the CpxR response regulator-CpxA sensor kinase two-component system regulates the expression of the pore-forming toxin α-hemolysin (HlyA) in response to environmental conditions. HlyA, in turn, is critical for fine-tuning the dynamics of host cell exfoliation and enhancing UPEC fitness during acute UTI.

Author contributions: K.N., T.J.H., and S.J.H. designed research; K.N., T.J.H., R.L.G., M.K., M.H., and J.B. performed research; K.N., T.J.H., T.L.R., and S.J.H. analyzed data; and K.N., T.J.H., M.H., K.D., and S.J.H. wrote the paper.

The authors declare no conflict of interest.

[1]Present address: Monsanto Company, Regulatory Organization, St. Louis, MO 63167.

[2]To whom correspondence should be addressed. Email: hultgren@wusm.wustl.edu.

This article contains supporting information online at www.pnas.org/lookup/suppl/doi:10.1073/pnas.1500374112/-/DCSupplemental.

of apoptotic signaling, which subsequently activates the effector Caspases, whereas the effector Caspases are responsible for degradation of the cellular contents during the demolition phase of apoptosis (18).

The proinflammatory Caspases (i.e., Caspase-1, Caspase-4) represent another group of Caspases that are not involved in the induction or execution of apoptosis (19). Caspase-1–dependent programmed cell death (also known as pyroptosis) is a host cell death pathway that is stimulated by a range of microbial infections (20–24), as well as noninfectious stimuli (25). Caspase-1 is activated by the canonical inflammasome, a multiprotein complex that forms in response to signals of cellular stress and/or infection. Canonical inflammasomes, such as NOD-like receptor family, pyrin domain containing 3 (NLRP3), NACHT, LRR, and PYD domains-containing protein 4 (NLRP4), and absent in melanoma 2, are cytosolic sensors that detect pathogens or danger signals and activate Caspase-1, leading to secretion of the proinflammatory cytokines interleukin (IL)-1β and IL-18 (26, 27). Recently, it was shown that mouse Caspase-11 (denoted here as mCaspase-11), which is the ortholog of human Caspase-4 (denoted here as hCaspase-4; 60% amino acid identity) (28), triggers proinflammatory cell death independent of canonical inflammasome assembly (29) and mediates innate detection and clearance of some natural cytosolic pathogens. The destruction of intracellular replication niches and the release of inflammatory cytokines and endogenous alarm signals may represent key mechanisms by which pyroptosis may contribute to the host's anti-infectious responses. Although mCaspase-11 activation also induces lysis of the host cell, mCaspase-11–dependent cell death has features that distinguish it from pyroptosis. Pyroptosis is accompanied by the release of mature IL-1β and IL-18 that are secreted by a Caspase-1–dependent mechanism (30). In contrast to pyroptosis, mCaspase-11 lacks the ability to cleave IL-1β and IL-18 by itself, because macrophages deficient in *Nlrp3* or *Casp1* still activate mCaspase-11 and initiate cell death but do not release mature IL-1β or IL-18. However, studies suggest that hCaspase-4 activation synergizes with the NLRP3 inflammasome pathway to coordinate Caspase-1 activation (31). Another difference between activation of canonical and noncanonical inflammasomes is in the release of IL-1α. The release of IL-1α requires cell lysis following mCaspase-11 activation (29). Given the importance of mCaspase-11 in pathogenesis, a better understanding of the mechanism of Caspase-11 activation is required.

In this work, we sought to elucidate the relationship between HlyA expression controlled by the response regulator (CpxR)-sensor kinase (CpxA) two-component signal transduction system (CpxRA), which senses periplasmic stress, and the exfoliation response induced during UPEC bladder infection. The CpxRA response regulator CpxR is known to modulate the expression of numerous genes (positively and negatively), including genes that encode periplasmic protein folding and trafficking factors (32). We found that UTI89Δ*cpxR* was attenuated in our murine model of cystitis. During acute infection, UTI89Δ*cpxR* induced a vigorous exfoliation of urothelial cells compared with UTI89. The membrane-embedded CpxA sensor intercepts the stress signal and responds by activating CpxR. We discovered that deletion of *cpxR* derepresses *hlyA* expression. Thus, UTI89Δ*cpxR* had significantly enhanced *hlyA* expression compared with UTI89, which led to an exacerbation of hCaspase-4/mCaspase-11–dependent cell death and early vigorous exfoliation of urothelial cells during acute infection, responses that were dependent upon the presence of HlyA. Thus, dysregulation of *hlyA* in UTI89Δ*cpxR* resulted in significant attenuation. The ability of UPEC to subvert an exfoliation response provides it access to the underlying epithelium, where it is able to establish QIRs that can serve as seeds for recurrent UTI (8). Thus, fine-tuning the expression of HlyA during acute bladder infection may serve to maximize UPEC persistence and give UPEC a fitness edge against the host innate inflammatory response.

Results

CpxR Regulates the Expression of Hemolysin. The CpxRA two-component system senses extracytoplasmic stress and responds by regulating the expression of genes to ensure the organism's survival. Previously, it was reported that CpxR negatively regulates hemolysin expression in *Xenorhabdus nematophila* (33). To assess CpxR regulation of HlyA in UPEC, we created a *cpxR* deletion in the human cystitis isolate UTI89 and used a blood agar plate assay to assess hemolytic activity. We found that the CpxR mutant (Δ*cpxR*) showed significantly larger zones of hemolytic clearance than WT UTI89 or a complemented strain in which the *cpxR* gene was introduced on the plasmid pTRC99A (pCpxR) (Fig. 1*A*). We saw no hemolysis with Δ*hlyA* or Δ*cpxR*Δ*hlyA* strains (Fig. 1*A*). These results suggest that CpxR influences the expression of *hlyA*. To assess CpxR regulation of *hlyA* further, we made a transcriptional fusion of the *hly* promoter to a GFP reporter gene (P*hlyA*::GFP). GFP expression was undetectable in the transformation of a parental vector that

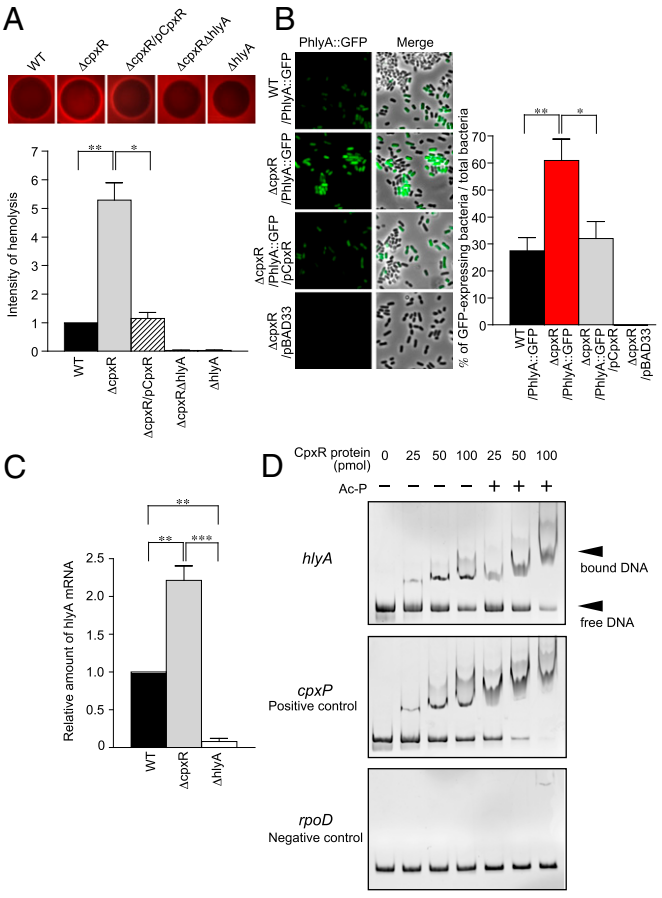

Fig. 1. *CpxR* regulates the expression of hemolysin. (*A*) Indicated strains were plated on blood agar plates and incubated overnight at 37 °C. The densitometry of hemolysis was performed using ImageJ. The densitometry of WT hemolysis is 1. Error bars represent ±SE. (*B*) In the absence or presence of WT CpxR, *hly* promoter-driven GFP expression in UTI89 WT and Δ*cpxR* was observed by fluorescence microscopy. Total bacteria were randomly picked from the fluorescence micrographs, and the percentages of GFP-expressing bacteria were determined. Percentages were based on a count of 100 bacteria, and the values are means ± SD from three independent experiments. (*C*) *HlyA* expression in UTI89 WT, Δ*cpxR*, and Δ*hlyA* was measured by qRT-PCR. The fold difference relative to the parent strain (UTI89 WT) was determined by the ΔΔCt method. (*D*) Mobility shift assays were performed with MBP-CpxR protein and a PCR product containing the *hlyA*, *cpxP*, *or rpoD* promoter region. Ac-P, acetyl phosphate. **P* < 0.05; ***P* < 0.01; ****P* < 0.001.

lacks the GFP gene into Δ*cpxR* (Fig. 1*B*). High GFP expression was observed in Δ*cpxR* P*hlyA*::GFP as determined by fluorescence microscopy analysis (Fig. 1*B*). When pCpxR was introduced, GFP expression decreased to levels similar to WT (Fig. 1*B*). Our quantitative RT-PCR (qRT-PCR) analyses confirmed that *hlyA* expression was increased in UTI89Δ*cpxR* compared with WT (Fig. 1*C*). Using an electrophoretic mobility shift assay (EMSA) (Fig. 1*D*), CpxR was found to bind to the *hlyCABD* promoter, as evidenced by a shift in the migration of the DNA after electrophoresis, with the amount of shifted probe correlated with increased amounts of CpxR (Fig. 1*D*). Together, these results strongly suggest that CpxR regulates *hlyA* expression through a direct interaction with the promoter.

Overexpression of HlyA Attenuates UPEC Virulence During Acute and Chronic Infection. Expression of HlyA in UPEC has been previously implicated in toxicity to urothelial cells in vitro (10, 11) and increased urothelial damage in vivo (12). We hypothesized that CpxR-dependent regulation of *hlyA* transcription fine-tunes HlyA protein levels, and thus host cell toxicity, to maximize bacterial colonization during acute bladder infection. To test this hypothesis, we infected C3H/HeN mice with mutant strains and evaluated bacterial loads in the bladder at 16 h post infection (hpi). We found that although Δ*hlyA* appeared to colonize the bladder as well as the WT parent, Δ*cpxR* and a WT strain overexpressing HlyA (WT/p*hlyCABD*) were both significantly attenuated (Fig. 2*A*). The complemented strain (Δ*cpxR*/pCpxR) or deletion of *hlyA* in the Δ*cpxR* mutant (Δ*cpxR*Δ*hlyA*) fully restored bladder virulence (Fig. 2*A*), indicating that the virulence phenotype correlated with higher levels of *hlyA* expression. The virulence phenotypes were not related to differences in the expression of UPEC type 1 pili, which has been shown to be critical for virulence (4), because all tested strains had identical type 1 piliation as measured by HA assays (Fig. S1*A*).

At 28 d postinfection (dpi), Δ*cpxR* and WT/p*hlyCABD* were also attenuated in their ability to cause chronic cystitis (Fig. 2*B*), which is defined by the presence of high-titer persistent bacteriuria ($>10^4$ cfu/mL) during the course of infection and bladder bacterial burdens of $>10^4$ cfu at death (34). Infection of C3H/HeN mice results in a bimodal distribution of colony-forming units at 28 dpi, reflecting mice that developed chronic cystitis and those mice that resolved infection or formed QIRs (34). Although WT UTI89 and the Δ*hlyA* strain caused similar incidences of chronic cystitis (Fig. 2*B*), there was a strong trend toward lower bacterial burdens in the absence of HlyA among those mice that resolved infection ($P = 0.07$, Mann–Whitney *U* test). Taken together, these results suggest that the development of chronic cystitis does not require hemolysin expression and that overexpression of hemolysin is detrimental to both acute and persistent UPEC infection of the bladder and may be repressed in the bladder niche. Based on these findings, we further evaluated the role of *hlyA* overproduction in the acute stages of infection.

We tested the effect of *hlyA* overproduction on the invasion of UPEC into bladder tissue by quantifying intracellular colony-forming unit and IBC formation as previously described in our murine model of cystitis (35). At 1 hpi, Δ*cpxR* was able to invade the urothelium similar to WT (Fig. 2*C*). However, the number of intracellular bacteria was significantly reduced at 3 and 16 hpi with either of the hemolysin-overexpressing strains: Δ*cpxR* and WT/p*hlyCABD* (Fig. 2*C*). In contrast, the intracellular population of Δ*cpxR*Δ*hlyA*, Δ*hlyA*, and Δ*cpxR*/pCpxR was not significantly different from WT at 3 and 16 hpi (Fig. 2*C*). In agreement with these results, Δ*cpxR* and WT/p*hlyCABD* showed a significant decrease in the invasion of human bladder epithelial cells (BECs) in vitro [urothelial line American Type Culture Collection (ATCC) HTB-9; also known as 5637], whereas all of the strains retained the ability to bind equivalently (Fig. S1 *B* and *C*). In our mouse model, IBC formation was quantitated at 6 hpi, marking the first round of IBC development. Significantly fewer IBCs were present in the Δ*cpxR* and WT/p*hlyCABD* strains compared with WT, whereas the number of IBCs present in the Δ*cpxR*/pCpxR, Δ*cpxR*Δ*hlyA*, and Δ*hlyA* strains was similar to WT (Fig. 2*D*).

We hypothesized that the attenuation of Δ*cpxR* may be due to the induction of an increased exfoliation response of superficial facet cells. Exfoliation is part of an innate host defense mechanism that facilitates the clearance of intracellular bacteria from the bladder. The luminal surface of the bladder is normally covered by binucleated superficial facet cells, which can be easily identified on the surface of whole-mount bladders stained with DAPI (36). Using this method, we observed a reduction in the abundance of binucleated urothelial cells at 6 hpi with either Δ*cpxR* or WT/p*hlyCABD* infection compared with infection with WT, Δ*cpxR*Δ*hlyA*, or Δ*hlyA* (Fig. 2*E*). The loss of binucleated cells was accompanied by an increase in the relative abundance of mononucleated cells (Fig. 2*E*). Furthermore, we analyzed Uroplakin III (UpIII) levels in homogenized bladder tissues by immunoblotting (Fig. 2*F*). UpIII is one of the main surface antigens present on the superficial facet cells of the urothelium and is a marker for terminal differentiation (37). Thus, the relative level of UpIII expression was used as an indication of the exfoliation response. We found similar UpIII levels in both uninfected and Δ*hlyA*-infected tissues (Fig. 2*F*), but significantly reduced UpIII levels in Δ*cpxR*- and WT/p*hlyCABD*-infected tissues (Fig. 2*F*). These results suggest that UPEC induces exfoliation of the bladder superficial facet cells and that overproduction of HlyA attenuates UPEC virulence during acute infection by triggering increased shedding of infected urothelial cells in the acute stages of disease.

UPEC Triggers Pyroptosis Through a Hemolysin-Dependent Pathway. We hypothesized that HlyA directly induces early urothelial cell death pathways. To test this hypothesis, a human BEC (urothelial) line [ATCC HTB-9 (5637)] was infected with WT, Δ*cpxR*, Δ*cpxR*/pCpxR, Δ*cpxR*Δ*hlyA*, Δ*hlyA*, or WT/p*hlyCABD* for the indicated times at a multiplicity of infection (MOI) of 10 and 100, and the release of cytoplasmic lactate dehydrogenase (LDH) into the medium was measured at 2 and 4 hpi (Fig. S2*A*). At 4 hpi, Δ*cpxR* and WT/p*hlyCABD* showed significantly enhanced urothelial cell death compared with both WT and Δ*cpxR*/pCpxR. The Δ*cpxR*Δ*hlyA* and Δ*hlyA* strains did not elicit any cytotoxicity, indicating that the cytotoxicity is hemolysin-dependent. To investigate whether Caspase pathways were involved in the urothelial cell death response, 5637 cells were treated with a Caspase-1/hCaspase-4 inhibitor. This inhibitor resulted in reduced cell death at 4 hpi in all strains to levels similar to the levels of Δ*hlyA*. In contrast, a Caspase-3 inhibitor did not significantly reduce death triggered by Δ*cpxR* and WT/p*hlyCABD* infection (Fig. 3*A*). These results indicate that urothelial cell death in vitro due to UPEC involves HlyA and activation of Caspase-1/hCaspase-4.

In addition to pyroptosis, Caspase-1 activation leads to the processing and release of mature IL-1β through a cytoplasmic complex known as the inflammasome (17). We thus assessed IL-1β production by 5637 cells infected with WT and mutant UTI89 strains (Fig. 3*B*). At 4 hpi, Δ*cpxR* and WT/p*hlyCABD* induced significantly higher IL-1β than WT UTI89 in a HlyA-dependent manner, because infection with either Δ*cpxR*Δ*hlyA* or Δ*hlyA* did not induce IL-1β secretion (Fig. 3*B*). Treatment of 5637 cells with a Caspase-1/hCaspase-4 inhibitor, but not a Caspase-3 inhibitor, significantly reduced IL-1β secretion triggered by Δ*cpxR* and WT/p*hlyCABD* infection (Fig. 3*B*). In addition to leading to cell death, hCaspase-4 has been shown to regulate the secretion of IL-1α, in an NLRP3/Caspase-1–independent manner (29). Accordingly, after 4 hpi, treatment of 5637 cells with a Caspase-1/hCaspase-4 inhibitor reduced IL-1α production in all strains to Δ*hlyA* levels. However, a Caspase-3 inhibitor had almost no effect on IL-1α production (Fig. 3*C*). Because Ac-YVAD-CHO

(EMD Chemicals, Inc.) inhibits both Caspase-1 and hCaspase-4 (29), these results indicate that either or both Caspase-1 and hCaspase-4 trigger IL-1α and IL-1β production in response to UPEC infection. We thus evaluated the effects of specifically knocking down Caspase-1 and Caspase-4 expression in 5637 cells using siRNAs that specifically target Caspase-1 and hCaspase-4 mRNA. Given that other bacterial hemolysins induce Caspase-1 activation via NLRP3 (15, 38) and that hCaspase-4 activation synergizes with the NLRP3 inflammasome pathway to coordinate Caspase-1 activation (31), we also targeted NLRP3 mRNA. As controls, we used scrambled siRNA. Immunoblotting demonstrated that expression of Caspase-1, hCaspase-4, and NLRP3 was each efficiently down-regulated by transfection with the respective siRNAs (Fig. S2*B*). When the control siRNA-transfected cells were infected with UPEC strains, they appeared intoxicated and round. However, in knockdown cells infected

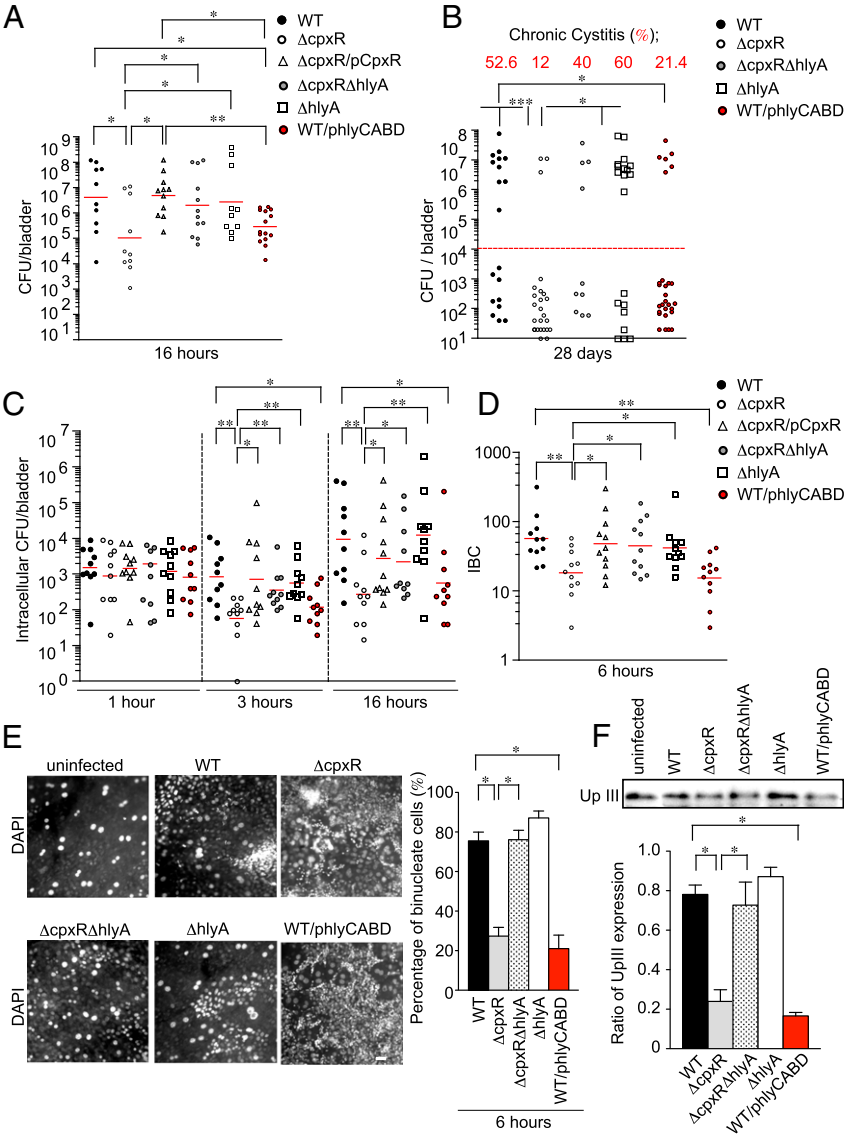

Fig. 2. Δ*cpxR* exhibits a colonization defect during acute infection. (*A*) Graphs depict the colony-forming units determined for the bladders of C3H/HeN mice ($n = 5$ for each group) infected with 10^7 cfu of the indicated strains. Mice were killed at 16 hpi, and excised bladders were homogenized and plated on LB plates. Colonies were counted to determine the number of colonized bacteria per organ. (*B*) Graph depicts the colony-forming units determined for the bladders of C3H/HeN mice ($n = 5$ for each group) infected with the indicated strains. Mice were killed at 28 d, and excised bladders were homogenized and plated on LB plates. (*C*) Graph depicts intracellular bacterial titers in the bladders of C3H/HeN mice ($n = 5$ for each group) infected with the indicated strains. Mice were killed at 1, 3, and 16 hpi, and bladders were removed, bisected, and incubated in gentamicin to kill extracellular bacteria. Gentamicin-treated bladders were washed, homogenized, and plated on LB plates, and colonies were counted to determine the number of intracellular colony-forming units per bladder. Data are representative of two independent experiments. Horizontal bars indicate the geometric mean. (*D*) Graph depicts IBCs enumerated via LacZ staining in bladders of C3H/HeN mice ($n = 5$ for each group) infected with the indicated strains. Mice were killed at 6 hpi, and bladders were removed, bisected, and stained with LacZ to quantify IBCs. Data are from two independent experiments. (*E*) Fixed whole-mounted bladders were stained with DAPI and imaged by fluorescence microscopy. C3H/HeN mice ($n = 3$ for each group) were inoculated transurethrally with the indicated strains, and bladders removed at 6 hpi. (Scale bar: 50 μm.) The percentage of urothelial cells was based on a unit area (600 μm^2). A value of 100 was set for uninfected bladders. Data are representative of three independent experiments. (*F*) C3H/HeN mice were infected with the indicated strains for 6 h. The homogenized bladder tissues were analyzed for the expression of UpIII by immunoblotting. The band intensity of UpIII was quantified and calculated in arbitrary units set to a value of 1 for uninfected bladder samples by the ImageJ application. $^*P < 0.05$; $^{**}P < 0.01$.

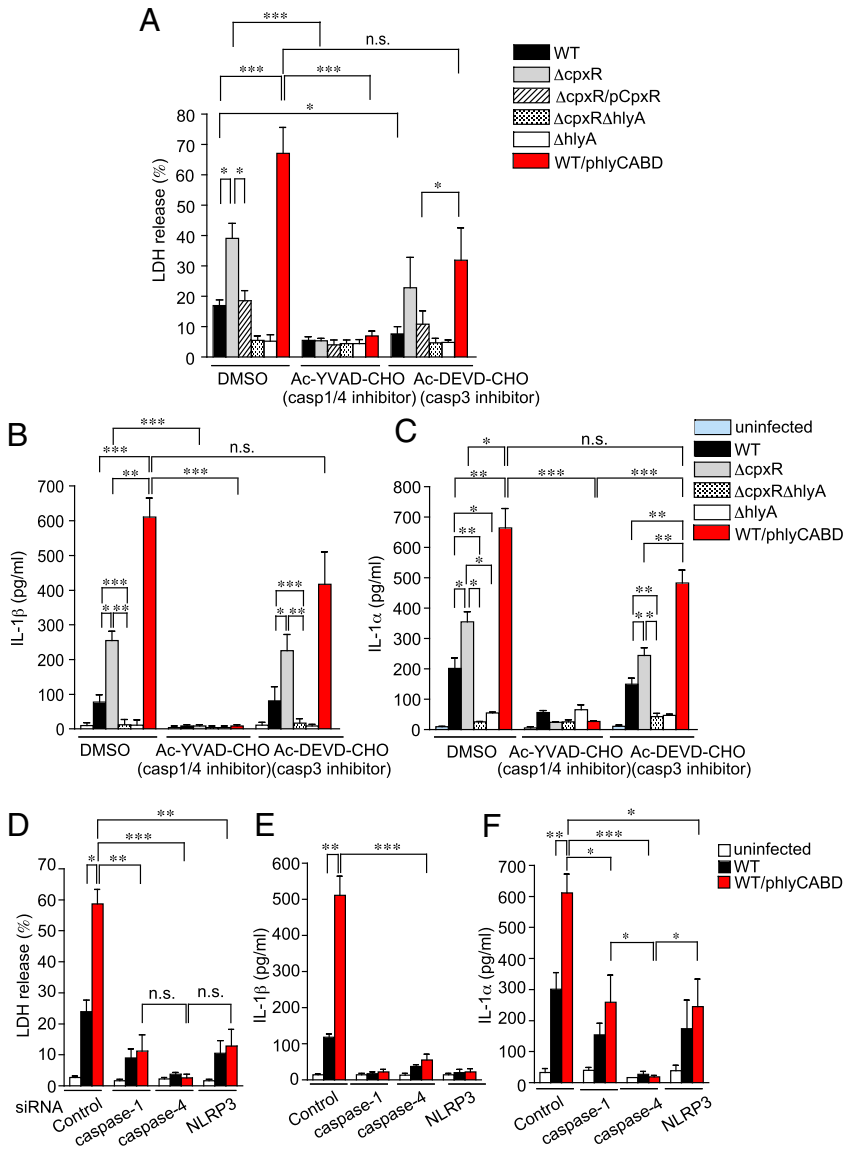

Fig. 3. Δ*cpxR* induces pyroptotic cell death in a hemolysin-dependent manner. (*A*) ATCC HTB-9 (5637) cells were treated for 1 h before and during infection with inhibitors specific for 10 μM Caspase-1/hCaspase-4 (Ac-YVAD-CHO) or Caspase-3 (Ac-DEVD-CHO). Cell death at an MOI of 10 for 4 hpi was determined by measuring LDH release in the presence of DMSO (vehicle control), Ac-YVAD-CHO, or Ac-DEVD-CHO. (*B*) 5637 cells were infected with the indicated strains in the presence of DMSO, Ac-YVAD-CHO, or Ac-DEVD-CHO. After 4 h, the amount of IL-1β in the culture medium was determined by ELISA. The depicted values are means ± SE from triplicate experiments. (*C*) 5637 cells were treated for 1 h before and during infection with inhibitors specific for Ac-YVAD-CHO or Ac-DEVD-CHO. After 4 h, the amount of IL-1α in the culture medium was determined by ELISA. The depicted values are means ± SE from triplicate experiments. (*D*) 5637 cells were transfected with siRNA against Caspase-1, Caspase-4, or NLRP3, or with scrambled siRNA. After 72 h, the cells were infected with UTI89-indicated strains for 4 h. Cell death was determined by measuring LDH release. The amount of IL-1β (*E*) and IL-1α (*F*) in the culture medium was determined by ELISA. $*P < 0.05$; $**P < 0.01$; $***P < 0.005$.

with UPEC, there was significantly reduced cell intoxication and rounding (Fig. S2*C*). We then infected siRNA-treated cells with WT or WT/p*hlyCABD* and measured the release of LDH, IL-1β, and IL-1α. Knockdown of Caspase-1 and NLRP3 expression significantly reduced LDH release and completely abolished secretion of IL-1β induced by UPEC infection (Fig. 3 *D* and *E*). Knockdown of hCaspase-4 expression completely eliminated LDH release induced by UPEC infection and greatly reduced the secretion of IL-1β triggered by WT/p*hlyCABD* infection (Fig. 3 *D* and *E*). Knockdown of hCaspase-4 expression, but not Caspase-1 or NLRP3 expression, abolished secretion of IL-1α in the cells infected with WT or WT/p*hlyCABD* (Fig. 3*F*). Thus, hCaspase-4 plays a central role in mediating the NLRP3-independent release of IL-1α. The effect of the hCaspase-4 siRNA in suppressing the release of IL-1β and cell death is possibly due to the ability of hCaspase-4 activation to synergize with the NLRP3 inflammasome pathway to coordinate Caspase-1 activation (31), in response to hemolysin-expressing UPEC infection.

UPEC HlyA Is Involved in Caspase-1 and NLRP3 Activation. We further assessed the expression of Caspase-1 in infected 5637 cells by immunofluorescence confocal microscopy (Fig. 4*A*). Staining with the fluorescent activity-based probe FLICA (FAM-YVAD-FMK; ImmunoChemistry Technologies) detects active Caspase-1/hCaspase-4 as indicated by cells with speckled, cytoplasmic FLICA staining (39) (Fig. 4*B*). As expected, speckled Caspase-1 staining was observed in 5637 cells infected with Δ*cpxR* and WT/p*hlyCABD*, whereas less

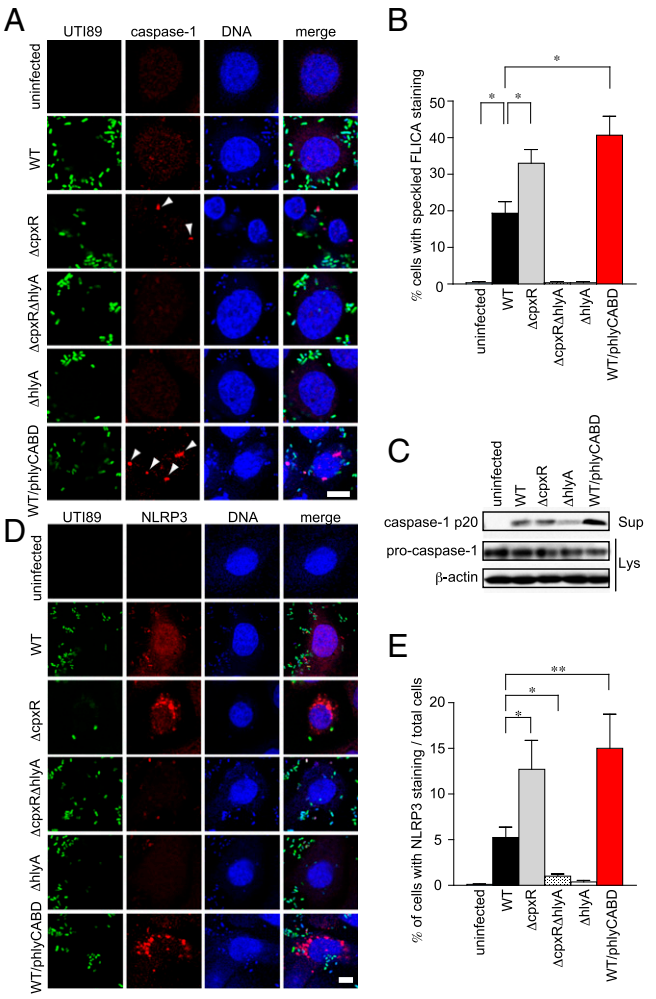

Fig. 4. HlyA triggers Caspase-1 activation and NLRP3 expression. (*A*) Immunofluorescence microscopy of 5637 cells infected for 4 h with the indicated UTI89 GFP-expressing strains. The 5637 cells were fixed and stained for Caspase-1 (red) and TOPRO3 (blue). Data are representative of three independent experiments. Arrowheads indicate Caspase-1 foci. (Scale bar: 10 μm.) (*B*) Percentage of cells with speckled, cytoplasmic FLICA staining. (*C*) 5637 cells were infected with UTI89-indicated strains for 4 h. The cells were analyzed for the expression of cleaved Caspase-1 in the supernatant (Sup) and procaspase-1, as well as for β-actin in the lysates (Lys) by immunoblotting. (*D*) Immunofluorescence microscopy of 5637 cells infected for 4 h with the indicated UTI89 GFP-expressing strains. The 5637 cells were fixed and stained for NLRP3 (red) and TOPRO3 (blue). Data are representative of three independent experiments. (Scale bar: 10 μm.) (*E*) 5637 cells infected with indicated strains were randomly picked from the immunofluorescence micrographs shown in *D*, and the percentages of cells showing NLRP3 staining were determined. Percentages were based on a count of 50 cells, and the values are means ± SD from three independent experiments. $*P < 0.05$; $**P < 0.01$.

intense Caspase-1 staining was observed in WT-infected cells (Fig. 4*A*). FLICA speckles were not observed in either Δ*cpxR*Δ*hlyA*- or Δ*hlyA*-infected cells (Fig. 4 *A* and *B*). Immunoblotting for the processed p20 subunit in culture supernatants of infected cells showed large amounts of processed p20 in the culture supernatant of 5637 cells infected with WT/p*hlyCABD*, but not in uninfected cells (Fig. 4*C*). Processed p20 was reduced in the supernatants of Δ*hlyA*-infected 5637 cells (Fig. 4*C*). Similarly, we found that NLRP3 aggregation triggered by Δ*cpxR* and WT/p*hlyCABD* infection was higher than in WT infection (Fig. 4 *D* and *F*). However, both Δ*cpxR*Δ*hlyA* and Δ*hlyA* failed to induce NLRP3 aggregation (Fig. 4 *D* and *F*). These results indicate that UPEC activates Caspase-1 and NLRP3 in a HlyA-dependent manner.

Overproduction of HlyA Increases Bladder Inflammasome Activation and IL-1β Secretion. To test whether enhanced Caspase-1/hCaspase-4 (mCaspase-11) activation and IL-1α/IL-1β secretion occurred in our murine model of infection, C3H/HeN mice were infected with 10^7 or 10^8 cfu of WT UPEC and bladder homogenates were collected at indicated time points for analysis of mRNA expression of Caspase pathway components (Fig. S3 and Table S1). Expression of the *mCasp11*, *Nlrp3*, *Il1*α, and *Il1*β genes was increased at early time points postinfection, whereas Casp1 transcript levels remained constant, rising only mildly at 24 hpi (Fig. S3). These results indicate that UPEC infection can elevate *mCasp11*, *Nlrp3*, *Il1*α, and *Il1*β gene expression in vivo, consistent with our in vitro results. Furthermore, the production of IL-1β was significantly higher in the bladder of mice infected with Δ*cpxR* than in the bladder of mice infected with WT, Δ*cpxR*Δ*hlyA*, or Δ*hlyA* at 24 hpi as assessed by ELISA (Fig. 5*A*). We also observed that cleaved Caspase-1 localized to infected BECs, with the highest expression levels in bladders infected with WT/p*hlyCABD*. Δ*cpxR* infection also induced higher levels of cleaved Caspase-1 compared with WT infection. These effects were not observed in either uninfected or Δ*hlyA*-infected bladders (Fig. 5 *B* and *C*). Using UTI89 strains containing a GFP expression plasmid (40), we observed cleaved Caspase-1 colocalized near areas of IBC formation in infected murine urothelial

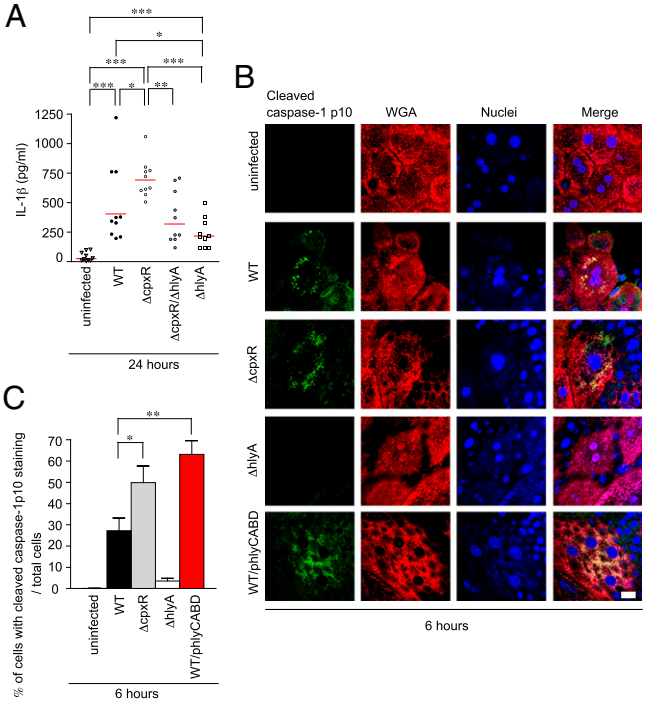

Fig. 5. Δ*CpxR* increased pyroptotic cell death by detecting the effects of hemolysin. (*A*) C3H/HeN mice ($n = 5$ for each group) infected with the indicated strains were killed at 24 h after infection. The amount of IL-1β in the homogenized bladder specimens was determined by ELISA. All statistics in panels are the results of a two-tailed Mann–Whitney *t* test. (*B*) C3H/HeN mice ($n = 2$ for each group) infected with the indicated UTI89 strains were killed at 6 h after infection. Fixed whole bladders were stained with anti–cleaved Caspase-1 p10 (green), WGA (red), and TOPRO3 (blue). Data are representative of three independent experiments. (Scale bar: 20 μm.) (*C*) Percentages of bladder umbrella cells showing punctate staining of Caspase-1 were determined as shown in *B*. The values are means ± SD from three independent experiments. $*P < 0.05$; $**P < 0.01$; $***P < 0.001$.

cells at 6 hpi (Fig. S4) for Δ*cpxR* and WT/phlyCABD. Taken together, these data suggest that overproduction of HlyA induces IL-1β secretion and Caspase-1 activation during acute infection.

Inhibition of Caspase-1/mCaspase-11 Restores Virulence of Δ*cpxR* in the Acute Infection Stages. Our data indicate that host immune responses involving Caspase1 and mCaspase 11 induce pyroptosis by detecting the effects of HlyA, resulting in the elimination of infected cells into the urine stream. To investigate interactions between Caspase-1/hCaspase-4–dependent pathways and UPEC virulence further, we inoculated C3H/HeN mice transurethrally with Caspase-1/mCaspase-11 inhibitor (Ac-YVAD-CMK; Bachem) 1 h before infection with WT or Δ*cpxR*, the inoculum of which also contained an additional dose of inhibitor. After 16 hpi, no significant difference was found between WT and Δ*cpxR* colonization in Caspase-1/mCaspase-11 inhibitor-treated mice (Fig. 6*A*), whereas the colonization by WT was significantly higher than colonization of Δ*cpxR* in the DMSO-treated control mice. Further, analysis of urine from DMSO-treated control mice at 16 hpi showed increased exfoliated urothelial cells and inflammatory cells in the urine of Δ*cpxR*-infected mice compared with WT-infected mice [Fig. 6 *B* (arrowheads) and *C*]. In addition, urinalysis showed that epithelial exfoliation and inflammatory infiltrates were reduced in the urine of Caspase-1/mCaspase-11 inhibitor-treated mice compared with DMSO-treated mice after infection with Δ*cpxR* (Fig. 6 *B* and *C*). These data suggest that the treatment of Caspase-1/mCaspase-11 inhibitor restores Δ*cpxR* acute virulence to WT levels. Together, our results suggest that HlyA induces Caspase-1/hCaspase-4–dependent cell death and that overproduction of HlyA, as occurs in Δ*cpxR*, attenuates the in vivo virulence of UPEC by overactivating these Caspase pathways.

Discussion

UPEC is known to encounter diverse host niches, including different locales of the urogenital tract, the gut, and the skin. To adapt successfully to these varied environments with their diverse selection pressures, a high degree of regulation of virulence gene expression is needed to promote bacterial persistence and dissemination. Two-component systems represent one mechanism by which bacteria are capable of regulating gene expression in response to changes in the external environment. A previous study demonstrated that the Cpx two-component system provides UPEC with a fitness advantage within the bladder, but the mechanism was not elucidated (41). In this study, we discovered that deletion of the response regulator *cpxR* gene in strain UTI89 (Δ*cpxR*) increased HlyA expression, resulting in a significant attenuation of virulence in the urinary tract. In its activated (phosphorylated) state, CpxR regulates the expression of several genes in response to envelope stress (32, 42). Deletion of *cpxR* led to the de-repression of *hlyA* regardless of the presence of envelope stress, suggesting that CpxR binds the promoter of *hlyA* at its resting state (as we have shown in Fig. 1*D*). Deletion of *hlyA* in the Δ*cpxR* strain fully restored virulence, indicating that the acute virulence defect of the Δ*cpxR* strain was primarily due to de-repression of HlyA. Consistent with these results, ectopic overexpression of the *hlyCABD* operon also was found to attenuate virulence to the same degree as Δ*cpxR*.

There are seemingly multifactorial pathways and signals leading to exfoliation, which has been shown to be a critical first line of defense against UPEC (4). Previously, a FimH-dependent apoptosis-like cell death was reported in C57BL6/J mice (4), and, here, we elucidated the HlyA-induced activation of Caspase-1 and mCaspase-11 in C3H/HeN mice. Thus, the mechanism of cell death in response to a uropathogen may vary depending on the genetic background of the host. *HlyA*-positive isolates have been shown to stimulate more rapid and extensive shedding of human BECs than isogenic *hlyA*-negative mutant strains (11, 12). HlyA-mediated exfoliation is, in part, due to its ability to trigger degradation of paxillin, a scaffold protein that can modulate the dynamics of cytoskeletal

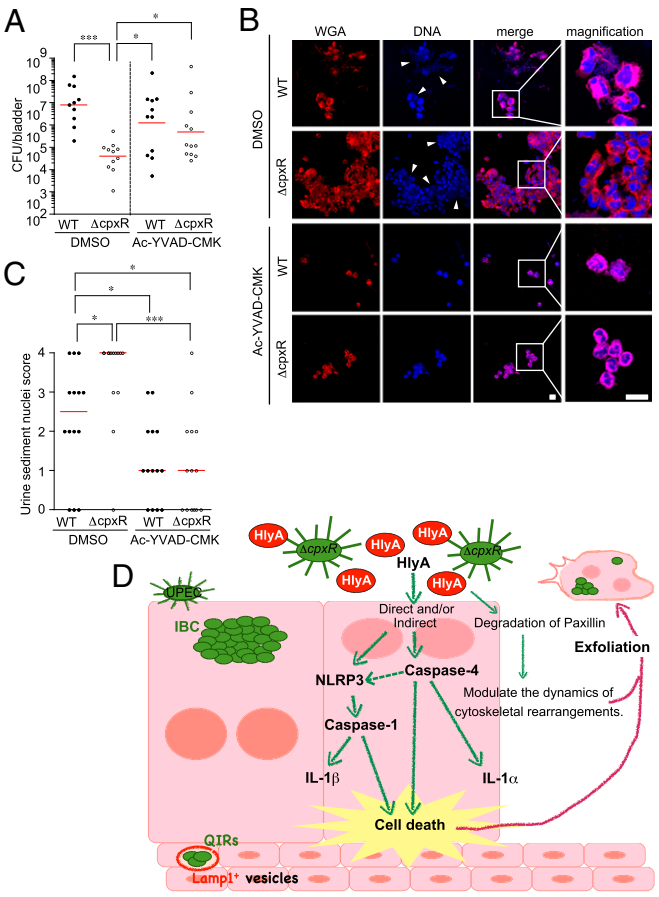

Fig. 6. Δ*CpxR* acute virulence is restored by inhibition of Caspase-1. (*A*) C3H/HeN mice ($n = 4$ for each group) were inoculated transurethrally with the indicated strains in the presence of DMSO or Ac-YVAD-CMK (Caspase-1/mCaspase-11 inhibitor). After 16 hpi, bladder specimens were homogenized and plated on LB plates. Colonies were counted to determine the number of bacteria per bladder. Data are representative of three independent experiments. All statistics shown are the results of a two-tailed Mann–Whitney *t* test. Horizontal bars indicate the geometric mean. (*B*) C3H/HeN mice ($n = 4$ for each group) were inoculated transurethrally with the indicated strains in the presence of DMSO or Ac-YVAD-CMK. After 16 hpi, urine sample were collected. Fixed urine samples were stained with WGA specific for the host cell surface (red) and TOPRO3 (blue). Arrowheads indicate bacteria. (Scale bar: 10 μm.) (*C*) Polymorphonuclear leukocytes and host nuclei scores of the urine sediments were determined at 16 hpi. Data are representative of three independent experiments. The statistics in *C* were determined by a two-tailed Mann–Whitney *t* test. The horizontal bars indicate the geometric mean. (*D*) Model for UPEC pathogenesis. UPEC HlyA triggers cell death and release of IL-1α and IL-1β. The dashed arrow indicates that it is not known how Caspase-4 synergizes with the assembled NLRP3 inflammasome to regulate Caspase-1 activation. $^*P < 0.05$; $^{***}P < 0.005$.

rearrangements (14). Here, we discovered that overexpression of the *hlyA* gene in UPEC triggers urothelial cell death and release of IL-1α via hCaspase-4 activation and Caspase-1–dependent IL-1β secretion via activation of the NLRP3 inflammasome pathway to orchestrate additional cell death. An inhibitor that blocks both Caspase-1 and murine Caspase-11 (ortholog of human Caspase-4) blocked hemolysin-triggered urothelial exfoliation and restored in vivo virulence to WT levels. Our data are consistent with a model whereby hCaspase-4–mediated cell death operates synergistically with the NLRP3/Caspase-1 inflammasome, because siRNA inhibition of hCaspase-4 in vitro reduced the levels of IL-1β secretion as well as abolishing IL-1α secretion. Inflammasome activation is thought to occur primarily in monocytic cells, such as macrophages;

however, it was recently shown that nonprofessional phagocytic cells, such as epithelial cells, could act as a front-line defense against intracellular pathogens by causing a Caspase-1–dependent cell death (43).

The exfoliation response likely represents a double-edged sword. On the one hand, rapid shedding of the superficial urothelial cells can eliminate infected cells that harbor IBCs. However, exfoliation also exposes underlying transitional cells, which can lead to the establishment of a QIR when accessed by UPEC. We previously demonstrated that C3H/HeN and other closely related inbred mouse strains are genetically susceptible to chronic cystitis because they mount severe inflammatory responses during acute infection that result in bladder immunopathology (34, 44). In this work, we found that deletion of *hlyA* does not affect the incidence of chronic cystitis, indicating that activation of the inflammasome and IL-1 signaling during early acute UPEC infection are each dispensable for the development of chronic cystitis. However, overexpression of HlyA during acute infection significantly reduces the incidence of chronic cystitis. Thus, an early robust urothelial exfoliation response seems to be protective against chronic cystitis, likely because the bacterial burden is reduced to levels where it is no longer able to persist and/or because less immunopathology is induced.

Although all *E. coli* harbors CpxRA, given its important role in mitigating envelope stress, only a very low percentage of nonpathogenic *E. coli* harbors *hlyA* (45). In contrast, ∼50% of UPEC strains harbor and express HlyA (46, 47) as part of their toxin repertoire. One of the reasons why *hlyA* is not harbored by all *E. coli* may be the toxin armamentarium of each strain. *E. coli* strains vary significantly in the types of toxins and microcins they harbor, and acquisition of several of these toxins may relieve the pressure of retaining *hlyA* in some cases. Alternatively, bladder mucosal remodeling as a consequence of chronic inflammation (48) may result in different predispositions, such that the requirements for virulence are likely not uniform among patients. With regard to clinical differences in the infections caused by HlyA-positive and -negative strains, reports indicate that UPEC strains that express HlyA cause more extensive tissue damage within the urinary tract and are associated with more severe clinical outcomes (49, 50). HlyA has also been shown to induce calcium oscillations in renal epithelial cells (51), and reports indicate a higher association of HlyA-positive UPEC with severe pyelonephritis (52, 53). Previous work also elucidated a role for HlyA in repressing host cell signaling; attenuating the viability, chemotaxis, and effector functions of host phagocytes like neutrophils and macrophages (54–57); and disrupting NF-κB signaling and expression of cytokine IL-6 (14). On the other hand, HlyA can also induce an inflammation response, as shown here. These complex factors, including host and bacterial genetics and prior history of UTIs, may have an impact on why ∼50% of UPEC strains encode HlyA.

Although we were unable to identify a beneficial role for HlyA expression conclusively during cystitis, there was a strong trend toward reduced bladder titers with the *hlyA* deletion mutant at 4 weeks postinfection in those mice that resolved bacteriuria during infection. UPEC has been shown to be able to survive in a Lamp-1^{+} vesicular compartment within bone marrow-derived macrophages (58) and in the bladder epithelium in mice that resolve acute infection (8) as part of a QIR that can seed later recurrent infection. Recently, it was reported that mCaspase-11 promotes the fusion of the *Legionella pneumophila* vacuole with lysosomes by modulating actin polymerization through cofilin (59). These results suggest that mCaspase-11 has other effector mechanisms besides cell death and NLRP3/Caspase-1–dependent cytokine maturation. The balance between cell death and phagosome–lysosome fusion is important for understanding both host defense and bacterial survival. Thus, a fine-tuned control of HlyA expression by Cpx may facilitate optimal exfoliation and other responses that allow UPEC to persist in the bladder epithelium.

In conclusion, UPEC HlyA triggers cell death and release of IL-1α and IL-1β via hCaspase-4 and/or Caspase-1 activation, which also leads to activation of the NLRP3 inflammasome pathway (Fig. 6*C*). The Cpx system is critical for fine-tuning this cytotoxic activity and enhancing UPEC fitness in vivo. We have discovered that Caspase-1/hCaspase-4–dependent innate immune processes play a critical role in the first line of defense against intracellular UPEC by detecting the effects of HlyA. Further detailed understanding of the host response to UPEC throughout the full time scale of infection and the interaction of the different host response systems is needed to understand this dynamic infection fully and will lead to elucidation of new and better ways to evaluate, treat, and prevent these common infections.

Materials and Methods

Host Cells. Human BECs, designated 5637 (ATCC HTB-9) cells, were obtained from the American Type Culture Collection and maintained in RPMI 1640 supplemented with heat-inactivated 10% (vol/vol) FBS at 37 °C in the presence of 5% CO_2.

Gene Cloning. UTI89 Δ*cpxR* and Δ*hlyA* were created using primer sets *cpxR*_Fwd (5′ CGTCTGATGACGTAATTTCTGCCTCGGAGGTATTTAAACAGTGTAGGCTGGAGCTGCTTC 3′) and *cpxR*_Rev (5′ AGCCAGAAGATGGCGAAGATGCGCGCGGTTAAGCTGCCTAATTCCGGGGATCCGTCGACC 3′) and primer sets *hlyA*_Fwd (5′ AAAAACAAGACAGATTTCAATTTTTCATTAACAGGTTAAGAGGTAATTAAGTGTAGGCTGGAGCTGCTTC 3′) and *hlyA*_Rev (5′ CTTATGTGGCACAGCCCAGTAAGATTGCTATCATTTAAATTAATATATTAATTCCGGGGATCCGTCGACC 3′), respectively.

The *cpxR* gene from UTI89 was amplified using primer sets Promoter_CpxR_Fwd_BamHI (5′ CGGGATCCGTTCGGTTAAACTTATGCCG 3′) and CpxR_Rev_EcoRI (5′ CGGAATTCTCATGAAGCAGAAACCATCAGATAGC 3′), and was ligated into pTrc99A to create a pCpxR strain. The HlyCABD promoter gene from UTI89 was amplified using primer sets Phly_Fwd_HindIII (5′ CCCAAGCTTATATTTTAGAGTATACTTGCGCACC 3′) and Phly_Rev_BamHI (5′ CGGGATCCTTGCGGTGGCAGGTTAAAAAAAG 3′), and was ligated into pBAD33 to create PhlyA::GFP. The IRDye 700 oligonucleotides were obtained from Integrated DNA Technologies. The labeling *hlyCABD* promoter oligos from UTI89 was amplified using primer sets IRD700_Fwd (5′ ATATTTTAGAGTATACTTGCGCACC 3′) and IRD700_Rev (5′ TTGCGGTGGCAGGTTAAAAAAAG 3′).

Bacterial Strains and Constructs. The UPEC strain used in this study was the human cystitis isolate UTI89 (4). UTI89 was transformed with a pANT4 plasmid to create the UTI89gfp strain. Deletion mutants were created using λ Red Recombinase (60). Antibiotic insertions were removed by transforming both ΔcpxR and ΔhlyA strains with pCP20 expressing the FLP recombinase (61). The pCpxR was created in pTrc99A (Invitrogen) by cloning *cpxR* downstream of the promoter. The p*PhlyA* was created by cloning the *hlyCABD* promoter into pSSH10-1 (62) and subcloning P*hlyA*::GFP into pBAD33 (62). UTI89 WT/phlyCABD was created using a plasmid, pACYC184, encoding the *hly* operon (hlyCABD) (63).

Blood Agar Plate Assay. UTI89 strains were streaked on blood agar plates, incubated overnight at 37 °C, and photographed digitally with a stereomicroscope (Olympus). Hemolytic activity was determined by densitometry analysis of the hemolytic halos using ImageJ (version 1.42; NIH).

HA Assays. HA analyses were performed on normalized cells (OD_{600} = 1) as described previously (64).

Inhibitors. For the Caspase inhibition experiments, the Caspase-1/hCaspase-4 inhibitor Ac-YVAD-CHO or the Caspase-3 inhibitor Ac-DEVD-CHO (both from EMD Chemicals, Inc.) was added to medium at 10 μM for 1 h before UTI89 infection.

Infection Assays and LDH Assay. Confluent, serum-starved 5637 cells in 24-well plates were infected with UTI89 strains at an MOI of 10. After 30 min, culture media were replaced by media with 120 μg/mL gentamicin sulfate (Sigma–Aldrich) to kill extracellular bacteria. Cells were further incubated for 1.5 and 3.5 h, the supernatants were collected, and the amounts of LDH were measured spectrophotometrically using a CytoTox 96 Non-Radioactive Cytotoxicity Assay Kit (Promega). Bacterial adherence and invasion were

assessed by lysing host cells with Triton X-100 and plating appropriate dilutions on LB agar plates.

siRNA Transfection. Caspase-1 (sc-29235), Caspase-4 (sc-56056), NLRP3 (sc-45469), and control (sc-37007; all from Santa Cruz Biotechnology) siRNA was transfected into 5637 cells using the siRNA Transfection Reagent (sc-29528; Santa Cruz Biotechnology). Forty-eight hours posttransfection, cells were analyzed for Caspase-1 and hCaspase-4 expression by immunoblotting. Transfected cells were infected with UTI89-WT and WT/phlyCABD for 4 h, and LDH release and the secretion of IL-1β and IL-1α were determined.

Immunoblotting. Cell culture supernatants were precipitated by trichloroacetic acid. Cells were lysed with 1% Nonidet P-40 lysis buffer. Immunoblot analysis was done with antibodies to human Caspase-1 (sc-622), human Caspase-4 (sc-56056), cleaved human Caspase-1 (sc-22163), NLRP3 (sc-134306), and β-actin (sc-1615; all from Santa Cruz Biotechnology). Bladder specimens were homogenized as described in in vivo infection of mice, and whole homogenized bladder tissues were analyzed using antibodies to UpIII (sc-15186; Santa Cruz Biotechnology). The band intensity of UpIII was quantified and calculated in arbitrary units set to a value of 1 for no infection by the ImageJ application.

Fluorescence Staining and Microscopy. The 5637 cells were seeded in a six-well plate and infected with UTI89 strains, which were transformed with a plasmid that constitutively expresses GFP, pANT (40), at an MOI of 10. After 4 h, 5637 cells were fixed for 15 min with 4% (wt/vol) paraformaldehyde in PBS and subjected to immunofluorescence staining with rabbit anti–Caspase-1 (Abcam) or anti-NLRP3 (R&D Systems). As a secondary antibody, Alexa Fluor 594 goat anti-rabbit IgG (Invitrogen) was used. Bladders were bisected, splayed, and fixed in 3% (wt/vol) paraformaldehyde for 1 h. Fixed whole bladders were stained with wheat germ agglutinin (WGA; Molecular Probes). Cleaved mouse Caspase-1 was stained with rabbit anti–Caspase-1 p10 (sc-514; Santa Cruz Biotechnology). Nuclei were stained with TOPRO3 (Molecular Probes) or DAPI (Invitrogen). For fluorescence and light microscopy, bacteria and host cells were visualized using a Zeiss fluorescence microscope.

FLICA Staining. The 5637 cells were seeded onto glass coverslips and infected with UTI89 strains at an MOI of 10 for 4 h. Coverslips were fixed and stained by FAM-YVAD-FMK (FLICA; ImmunoChemistry Technologies). Medium was replaced with fresh RPMI-1640 containing 5 μM FLICA 1 h before fixation.

EMSA. EMSAs were performed as previously described (65) using a purified MBP-CpxR fusion protein and a PCR-amplified region of the *hly* operon 400 bp upstream of the *hlyC* ATG, from c4829152 to c4828752 of the *E. coli* UTI89 chromosome, complete genome. Using an IRDye EMSA reagents kit (Odyssey Infrared EMSA Kit; LI-COR), a binding reaction was carried out for 30 min at room temperature, and samples were then loaded onto 5% (wt/vol) polyacrylamide gels. Following electrophoresis, the gels were imaged with an Odyssey CLx Infrared Imaging System (LI-COR).

Inoculations of Mice. C3H/HeN mice were obtained from Harlan Sprague Dawley. Mice were anesthetized and inoculated via transurethral catheterization with 50 μL of bacterial suspension (10^7 cfu) in PBS. At the times indicated, mice were killed and bladders were aseptically removed and processed for confocal microscopy, lacZ staining (35), or colony-forming unit titration. On 28 dpi, we plated WT/phlyCABD on LB agar or LB chloramphenicol (50 μg/mL) to confirm that the titers were the same. Standard gentamicin assays were done to determine the number of intracellular bacteria in the bladder (7). To test the effect of Caspase-1 on bacterial colonization, mice were inoculated transurethrally with 50 μL of a 1 mM solution of Caspase-1/mCaspase-11 inhibitor, Ac-YVAD-CMK (Bachem) in PBS 1 h before inoculation, with UTI89 strains containing an additional dose of the inhibitor. All analyses were performed in adult female mice (n = 4–7 mice per experimental group for all experiments).

Ethics Statement. Experiments were performed using protocols approved by the Animal Studies Committee of the Washington University School of Medicine (Animal Welfare Assurance no. A-3381-01). Mice were maintained under specified pathogen-free conditions in a barrier facility and under a strict 12-h light cycle.

Urine Collection and Urine Sediment Analysis. Urine was collected at 16 hpi by applying suprapubic pressure with proper restraint and collecting the urine stream in sterile 1.5-mL Eppendorf tubes. Urine sediments were obtained by cytocentrifuging 100 μL of a 1:10 dilution of the collected urine onto glass slides and were stained with WGA and TOPRO3. Stained urine sediments were examined by confocal microscopy, and the average number of host cell nuclei per field at magnification of 400× [high-powered field (hpf)] was calculated from counting five fields. A semiquantitative scoring system was created to facilitate analysis: 0, less than 1 nucleus per hpf; 1, 1–5 nuclei per hpf; 2, 6–10 nuclei per hpf; 3, 11–20 nuclei per hpf; 4, >20 nuclei per hpf.

Cytokine Detection and ELISAs. Confluent monolayers of 5637 cells grown overnight in 24-well plates were infected with UTI89, UTI89Δ*cpxR*, UTI89Δ*cpxR*Δ*hlyA*, or UTI89Δ*hlyA* (MOI of 10) for 4 h. Concentrations of IL-1β or IL-1α in the collected supernatants were determined by an ELISA development kit (DuoSet; R&D Systems). Bladder specimens were homogenized as described for in vivo infection of mice, and concentrations of IL-1β in the bladder homogenates were determined by the ELISA development kit.

qRT-PCR Assay. RNA was extracted from bacteria or infected mouse bladders at indicated time points, as well as from PBS mock-infected mouse bladders, using an RNeasy Plus Mini kit (QIAGEN) and reverse-transcribed with iScript Reverse Transcription Supermix (Bio-Rad). For qRT-PCR assay, 1 μL of 12.5 ng/μL cDNA was used with primers specific to *mCasp1*, *mCasp11*, *mNlrp3*, *mIl1α*, *mIl1β*, and *hlyA* [designed using the Roche Universal Probe Library Assay Design tool and the Primer Design online tool (GenScript)] and iQ SYBR Green supermix according to the manufacturer's instructions (Bio-Rad). Expression values were normalized to 16S or 18S expression levels, and the fold difference relative to the parent strain (UTI89 WT) or mock-infected bladders, respectively, was determined by the cycle threshold (ΔΔCt) method (66). Each sample was run in triplicate, and average Ct values were calculated.

Statistical Analysis. Statistical analysis was performed using the Mann–Whitney t test (two-tailed), Fisher's exact test (two-tailed), or unpaired Student's t test. A value of $P < 0.05$ was considered to be significant.

ACKNOWLEDGMENTS. We thank Chia Hung for contributing to making the *cpxR* deletion mutant. We thank Matthew A. Mulvey for providing the *hly* overexpression strain. We thank members of the S.J.H. laboratory for their insightful editorial comments and suggestions. This work was supported by NIH Grants DK51406, DK64540, and U01 AI095542 (to S.J.H.); a Mentored Clinical Scientist Research Career Development Award K08 AI083746 to (T.J.H.); an Alexander Berg Fellowship (to K.N.); Canadian Institute of Health Research Operating Grant 97819; and an Alberta Innovates Health Research Senior Scholar Award (to T.L.R.).

1. Ronald A (2003) The etiology of urinary tract infection: Traditional and emerging pathogens. *Dis Mon* 49(2):71–82.
2. Song J, et al. (2009) TLR4-mediated expulsion of bacteria from infected bladder epithelial cells. *Proc Natl Acad Sci USA* 106(35):14966–14971.
3. Anderson GG, et al. (2003) Intracellular bacterial biofilm-like pods in urinary tract infections. *Science* 301(5629):105–107.
4. Mulvey MA, et al. (1998) Induction and evasion of host defenses by type 1-piliated uropathogenic Escherichia coli. *Science* 282(5393):1494–1497.
5. Justice SS, et al. (2004) Differentiation and developmental pathways of uropathogenic Escherichia coli in urinary tract pathogenesis. *Proc Natl Acad Sci USA* 101(5): 1333–1338.
6. Mulvey MA, Schilling JD, Martinez JJ, Hultgren SJ (2000) Bad bugs and beleaguered bladders: Interplay between uropathogenic Escherichia coli and innate host defenses. *Proc Natl Acad Sci USA* 97(16):8829–8835.
7. Mulvey MA, Schilling JD, Hultgren SJ (2001) Establishment of a persistent Escherichia coli reservoir during the acute phase of a bladder infection. *Infect Immun* 69(7): 4572–4579.
8. Mysorekar IU, Hultgren SJ (2006) Mechanisms of uropathogenic Escherichia coli persistence and eradication from the urinary tract. *Proc Natl Acad Sci USA* 103(38): 14170–14175.
9. Hannan TJ, et al. (2008) LeuX tRNA-dependent and -independent mechanisms of Escherichia coli pathogenesis in acute cystitis. *Mol Microbiol* 67(1):116–128.
10. Mobley HL, et al. (1990) Pyelonephritogenic Escherichia coli and killing of cultured human renal proximal tubular epithelial cells: Role of hemolysin in some strains. *Infect Immun* 58(5):1281–1289.
11. Smith YC, Grande KK, Rasmussen SB, O'Brien AD (2006) Novel three-dimensional organoid model for evaluation of the interaction of uropathogenic Escherichia coli with terminally differentiated human urothelial cells. *Infect Immun* 74(1):750–757.
12. Smith YC, Rasmussen SB, Grande KK, Conran RM, O'Brien AD (2008) Hemolysin of uropathogenic Escherichia coli evokes extensive shedding of the uroepithelium and hemorrhage in bladder tissue within the first 24 hours after intraurethral inoculation of mice. *Infect Immun* 76(7):2978–2990.
13. Welch RA (1991) Pore-forming cytolysins of gram-negative bacteria. *Mol Microbiol* 5(3):521–528.

14. Dhakal BK, Mulvey MA (2012) The UPEC pore-forming toxin α-hemolysin triggers proteolysis of host proteins to disrupt cell adhesion, inflammatory, and survival pathways. *Cell Host Microbe* 11(1):58–69.
15. Craven RR, et al. (2009) Staphylococcus aureus alpha-hemolysin activates the NLRP3-inflammasome in human and mouse monocytic cells. *PLoS ONE* 4(10):e7446.
16. Strasser A, O'Connor L, Dixit VM (2000) Apoptosis signaling. *Annu Rev Biochem* 69: 217–245.
17. Lamkanfi M, Dixit VM (2010) Manipulation of host cell death pathways during microbial infections. *Cell Host Microbe* 8(1):44–54.
18. Cryns V, Yuan J (1998) Proteases to die for. *Genes Dev* 12(11):1551–1570.
19. Li P, et al. (1995) Mice deficient in IL-1 beta-converting enzyme are defective in production of mature IL-1 beta and resistant to endotoxic shock. *Cell* 80(3):401–411.
20. Molofsky AB, et al. (2006) Cytosolic recognition of flagellin by mouse macrophages restricts Legionella pneumophila infection. *J Exp Med* 203(4):1093–1104.
21. Mariathasan S, Weiss DS, Dixit VM, Monack DM (2005) Innate immunity against Francisella tularensis is dependent on the ASC/caspase-1 axis. *J Exp Med* 202(8): 1043–1049.
22. Lara-Tejero M, et al. (2006) Role of the caspase-1 inflammasome in Salmonella typhimurium pathogenesis. *J Exp Med* 203(6):1407–1412.
23. Raupach B, Peuschel SK, Monack DM, Zychlinsky A (2006) Caspase-1-mediated activation of interleukin-1beta (IL-1beta) and IL-18 contributes to innate immune defenses against Salmonella enterica serovar Typhimurium infection. *Infect Immun* 74(8):4922–4926.
24. Sansonetti PJ, et al. (2000) Caspase-1 activation of IL-1beta and IL-18 are essential for Shigella flexneri-induced inflammation. *Immunity* 12(5):581–590.
25. Frantz S, et al. (2003) Targeted deletion of caspase-1 reduces early mortality and left ventricular dilatation following myocardial infarction. *J Mol Cell Cardiol* 35(6): 685–694.
26. Miao EA, Rajan JV, Aderem A (2011) Caspase-1-induced pyroptotic cell death. *Immunol Rev* 243(1):206–214.
27. Fantuzzi G, Dinarello CA (1999) Interleukin-18 and interleukin-1 beta: Two cytokine substrates for ICE (caspase-1). *J Clin Immunol* 19(1):1–11.
28. Kang SJ, et al. (2000) Dual role of caspase-11 in mediating activation of caspase-1 and caspase-3 under pathological conditions. *J Cell Biol* 149(3):613–622.
29. Kayagaki N, et al. (2011) Non-canonical inflammasome activation targets caspase-11. *Nature* 479(7371):117–121.
30. Keller M, Rüegg A, Werner S, Beer HD (2008) Active caspase-1 is a regulator of unconventional protein secretion. *Cell* 132(5):818–831.
31. Rathinam VA, et al. (2012) TRIF licenses caspase-11-dependent NLRP3 inflammasome activation by gram-negative bacteria. *Cell* 150(3):606–619.
32. Ruiz N, Silhavy TJ (2005) Sensing external stress: Watchdogs of the Escherichia coli cell envelope. *Curr Opin Microbiol* 8(2):122–126.
33. Herbert EE, Cowles KN, Goodrich-Blair H (2007) CpxRA regulates mutualism and pathogenesis in Xenorhabdus nematophila. *Appl Environ Microbiol* 73(24):7826–7836.
34. Hannan TJ, Mysorekar IU, Hung CS, Isaacson-Schmid ML, Hultgren SJ (2010) Early severe inflammatory responses to uropathogenic E. coli predispose to chronic and recurrent urinary tract infection. *PLoS Pathog* 6(8):e1001042.
35. Justice SS, Lauer SR, Hultgren SJ, Hunstad DA (2006) Maturation of intracellular Escherichia coli communities requires SurA. *Infect Immun* 74(8):4793–4800.
36. Blango MG, Ott EM, Erman A, Veranic P, Mulvey MA (2014) Forced resurgence and targeting of intracellular uropathogenic Escherichia coli reservoirs. *PLoS ONE* 9(3): e93327.
37. Wu XR, Sun TT (1993) Molecular cloning of a 47 kDa tissue-specific and differentiation-dependent urothelial cell surface glycoprotein. *J Cell Sci* 106(Pt 1):31–43.
38. Muñoz-Planillo R, Franchi L, Miller LS, Núñez G (2009) A critical role for hemolysins and bacterial lipoproteins in Staphylococcus aureus-induced activation of the Nlrp3 inflammasome. *J Immunol* 183(6):3942–3948.
39. Broz P, von Moltke J, Jones JW, Vance RE, Monack DM (2010) Differential requirement for Caspase-1 autoproteolysis in pathogen-induced cell death and cytokine processing. *Cell Host Microbe* 8(6):471–483.
40. Lee AK, Falkow S (1998) Constitutive and inducible green fluorescent protein expression in Bartonella henselae. *Infect Immun* 66(8):3964–3967.
41. Debnath I, et al. (2013) The Cpx stress response system potentiates the fitness and virulence of uropathogenic Escherichia coli. *Infect Immun* 81(5):1450–1459.
42. Hunke S, Keller R, Müller VS (2012) Signal integration by the Cpx-envelope stress system. *FEMS Microbiol Lett* 326(1):12–22.
43. Jorgensen I, et al. (2011) The Chlamydia protease CPAF regulates host and bacterial proteins to maintain pathogen vacuole integrity and promote virulence. *Cell Host Microbe* 10(1):21–32.
44. Hannan TJ, et al. (2012) Host-pathogen checkpoints and population bottlenecks in persistent and intracellular uropathogenic Escherichia coli bladder infection. *FEMS Microbiol Rev* 36(3):616–648.
45. Cavalieri SJ, Bohach GA, Snyder IS (1984) Escherichia coli alpha-hemolysin: Characteristics and probable role in pathogenicity. *Microbiol Rev* 48(4):326–343.
46. Brauner A, Katouli M, Tullus K, Jacobson SH (1990) Production of cytotoxic necrotizing factor, verocytotoxin and haemolysin by pyelonephritogenic Escherichia coli. *Eur J Clin Microbiol Infect Dis* 9(10):762–767.
47. Siegfried L, Kmetová M, Puzová H, Molokácová M, Filka J (1994) Virulence-associated factors in Escherichia coli strains isolated from children with urinary tract infections. *J Med Microbiol* 41(2):127–132.
48. Hannan TJ, et al. (2014) Inhibition of Cyclooxygenase-2 Prevents Chronic and Recurrent Cystitis. *EBioMedicine* 1(1):46–57.
49. Johnson JR (1991) Virulence factors in Escherichia coli urinary tract infection. *Clin Microbiol Rev* 4(1):80–128.
50. Marrs CF, Zhang L, Foxman B (2005) Escherichia coli mediated urinary tract infections: Are there distinct uropathogenic E. coli (UPEC) pathotypes? *FEMS Microbiol Lett* 252(2):183–190.
51. Uhlén P, et al. (2000) Alpha-haemolysin of uropathogenic E. coli induces Ca2+ oscillations in renal epithelial cells. *Nature* 405(6787):694–697.
52. Jacobson SH, Hylander B, Wretlind B, Brauner A (1994) Interleukin-6 and interleukin-8 in serum and urine in patients with acute pyelonephritis in relation to bacterial-virulence-associated traits and renal function. *Nephron* 67(2):172–179.
53. O'Hanley P, Lalonde G, Ji G (1991) Alpha-hemolysin contributes to the pathogenicity of piliated digalactoside-binding Escherichia coli in the kidney: Efficacy of an alpha-hemolysin vaccine in preventing renal injury in the BALB/c mouse model of pyelonephritis. *Infect Immun* 59(3):1153–1161.
54. Cavalieri SJ, Snyder IS (1982) Effect of Escherichia coli alpha-hemolysin on human peripheral leukocyte function in vitro. *Infect Immun* 37(3):966–974.
55. Wiles TJ, Bower JM, Redd MJ, Mulvey MA (2009) Use of zebrafish to probe the divergent virulence potentials and toxin requirements of extraintestinal pathogenic Escherichia coli. *PLoS Pathog* 5(12):e1000697.
56. Gadeberg OV, Hacker J, Orskov I (1989) Role of alpha-hemolysin for the in vitro phagocytosis and intracellular killing of Escherichia coli. *Zentralbl Bakteriol* 271(2): 205–213.
57. Russo TA, et al. (2005) E. coli virulence factor hemolysin induces neutrophil apoptosis and necrosis/lysis in vitro and necrosis/lysis and lung injury in a rat pneumonia model. *Am J Physiol Lung Cell Mol Physiol* 289(2):L207–L216.
58. Bokil NJ, et al. (2011) Intramacrophage survival of uropathogenic Escherichia coli: Differences between diverse clinical isolates and between mouse and human macrophages. *Immunobiology* 216(11):1164–1171.
59. Akhter A, et al. (2012) Caspase-11 promotes the fusion of phagosomes harboring pathogenic bacteria with lysosomes by modulating actin polymerization. *Immunity* 37(1):35–47.
60. Murphy KC, Campellone KG (2003) Lambda Red-mediated recombinogenic engineering of enterohemorrhagic and enteropathogenic E. coli. *BMC Mol Biol* 4:11.
61. Cherepanov PP, Wackernagel W (1995) Gene disruption in Escherichia coli: TcR and KmR cassettes with the option of Flp-catalyzed excision of the antibiotic-resistance determinant. *Gene* 158(1):9–14.
62. Wright KJ, Seed PC, Hultgren SJ (2005) Uropathogenic Escherichia coli flagella aid in efficient urinary tract colonization. *Infect Immun* 73(11):7657–7668.
63. Welch RA, Dellinger EP, Minshew B, Falkow S (1981) Haemolysin contributes to virulence of extra-intestinal E. coli infections. *Nature* 294(5842):665–667.
64. Hultgren SJ, Schwan WR, Schaeffer AJ, Duncan JL (1986) Regulation of production of type 1 pili among urinary tract isolates of Escherichia coli. *Infect Immun* 54(3): 613–620.
65. Vogt SL, Evans AD, Guest RL, Raivio TL (2014) The Cpx envelope stress response regulates and is regulated by small noncoding RNAs. *J Bacteriol* 196(24):4229–4238.
66. Pfaffl MW (2001) A new mathematical model for relative quantification in real-time RT-PCR. *Nucleic Acids Res* 29(9):e45.